

1 **RESPONSE TO COMMENTS OF THE ASSOCIATE EDITOR**

2 **Associate Editor comments:** Thank you for replying to the reviewers comments. The revised
3 manuscript is much improved, but I would like you to 1)ensure that Figure 6 is cited in the
4 text and 2)comment on the importance of the single high value to the correlation in 6b. It
5 appears to me that the data point drives the relationship, which should be discussed in the
6 text. The manuscript should be acceptable for publication after addressing that point.

7 **Author's response:**

8 We thank the Associate Editor for his inputs.

9 1) Figure 6 is cited in the text in the revised version.

10 2) We assume the editor is referring to Figure 5b. We have addressed this point in the
11 revised manuscript.

12

13

14

15

16

17

18

19

20

21

22

23

24

25

26

27

28 **AUTHOR'S CHANGES IN THE MANUSCRIPT**

29 **Isotopic composition of nitrate and particulate organic matter in a**
30 **pristine dam-reservoir of western India: Implications for**
31 **biogeochemical processes**

32 Pratirupa Bardhan, S.W.A. Naqvi, Supriya G. Karapurkar, Damodar M. Shenoy, Siby Kurian,
33 Hema Naik.

34 CSIR-National Institute of Oceanography, Dona Paula, Goa:403004, India.

35 *Correspondence to:* P.Bardhan (pratirupabardhan@gmail.com)

36

37

38

39

40

41

42

43

44

45

46

47

48

49

50

51

52 **Abstract:**

53
54 Isotopic composition of nitrate ($\delta^{15}\text{N}$ and $\delta^{18}\text{O}$) and particulate organic matter (POM) ($\delta^{15}\text{N}$
55 and $\delta^{13}\text{C}$) were measured in Tillari Reservoir, located at the foothills of the Western Ghats,
56 Maharashtra, western India. The reservoir that is stratified during spring-summer and autumn
57 seasons but gets vertically mixed during the Southwest Monsoon (SWM) and winter is
58 characterized by diverse redox nitrogen transformations in space and time. The $\delta^{15}\text{N}$ and $\delta^{18}\text{O}$
59 values of nitrate were low ($\delta^{15}\text{N} = 2\text{-}10\text{‰}$, $\delta^{18}\text{O} = 5\text{-}8\text{‰}$) during normoxic conditions but
60 increased gradually (highest $\delta^{15}\text{N}=27\text{‰}$, $\delta^{18}\text{O}=29\text{‰}$) when anoxic conditions facilitated
61 denitrification in the hypolimnion during spring-early summer. Once nitrate was fully utilized
62 and sulphidic conditions set in, NH_4^+ became the dominant inorganic N species, with $\delta^{15}\text{N}$
63 ranging from 1.3 to 2.6‰. Low $\delta^{15}\text{N}$ ($\sim\text{-}5\text{‰}$) and $\delta^{13}\text{C}$ ($\text{-}37\text{‰}$ to $\text{-}32\text{‰}$) of POM co-
64 occurring with high NH_4^+ and CH_4 in sulphidic bottom waters were probably the consequence
65 of microbial chemosynthesis. Assimilation of nitrate in the epilimnion was the major
66 controlling process on the N-isotopic composition of POM ($\delta^{15}\text{N} = 2 - 6 \text{‰}$). Episodic low
67 $\delta^{15}\text{N}$ values of POM ($\text{-}2$ to 0‰) during early summer coinciding with the absence of nitrate
68 might arise from N-fixation, although further work is required to confirm the hypothesis.
69 $\delta^{13}\text{C}$ -POM in the photic zone ranged between $\text{-}29\text{‰}$ and $\text{-}27\text{‰}$ for most parts of the year.
70 The periods of mixing were characterized by uniform $\delta^{15}\text{N}\text{-NO}_3^-$ and $\delta^{18}\text{O}\text{-NO}_3^-$ at all depths.
71 Higher POM (particulate organic carbon (POC) as well as particulate organic nitrogen
72 (PON)) contents and C/N values with lower $\delta^{13}\text{C}$ -POM during the SWM point to
73 allochthonous inputs. Overall, this study, the first of its kind in the Indian subcontinent,
74 provides an insight into biogeochemistry of Indian reservoirs, using stable carbon and
75 nitrogen isotopes as a tool, where the monsoons play an important role in controlling vertical
76 mixing and dynamics of carbon and nutrients.

77

78 **1.Introduction:**

79 Nitrogen is an essential macronutrient the availability of which often limits primary
80 production in aquatic ecosystems. It is a polyvalent element that undergoes redox
81 transformation between the terminal oxidation states of +5 and -3. These transformations
82 involve isotopic fractionation to varying degrees, and so natural abundance of stable isotopes
83 (¹⁵N and ¹⁴N) in various N species provides useful insight into nitrogen cycling besides its
84 sources/sinks in the oceanic (Altabet, 1988; Sigman et al., 2005), coastal (Thunell et al.,
85 2004; Hu et al., 2015) and estuarine (Cifuentes et al, 1988; Savoye et al., 2012) water-bodies
86 and sediments. Studies have also been undertaken in freshwater systems like lakes (Pang and
87 Nriagu, 1977; Chen et al., 2014) and reservoirs (Chen and Jia, 2009; Junet et al., 2009). Some
88 of the best studied freshwater ecosystems in this regard are Lake Lugano at the Swiss-Italian
89 border, Lake Kinneret in Israel and Lake Superior in the USA.

90 In the eutrophic Lake Lugano, the highly depleted $\delta^{13}\text{C}$ and $\delta^{15}\text{N}$ of the near-bottom POM
91 established the active presence of methanotrophic bacteria during suboxic conditions
92 (Lehmann et al., 2004). Seasonal changes in nitrogen species were reflected in the isotopic
93 composition of particulate organic matter (POM) and dissolved inorganic nitrogen (DIN)
94 compounds in Lake Kinneret (Hadas et al., 2009). Various processes like nitrification,
95 denitrification and N₂-fixation were identified with the help of the N isotopes. In Lake
96 Superior, based on nitrate isotopic studies it was possible to identify the increasing inputs of
97 reduced N to the lake and its subsequent nitrification to be the cause behind a century-long
98 increase in the nitrate inventory of the lake, ruling out atmospheric deposition as the other
99 probable cause (Finlay et al., 2007).

100 There are a large number of natural freshwater lakes as well as man-made reservoirs in India.
101 In fact, India has the third-highest number of dams (around 4300) in the world, after China
102 and USA. However, these systems have not been well investigated for biogeochemical

103 cycling.. In the very first study of its kind, Narvenkar et al. (2013) sampled eight dam-
104 reservoirs spread across India and observed strong thermal stratification during summer in all
105 reservoirs. Six of these reservoirs were found to experience varying degrees of oxygen
106 depletion in the hypolimnia, ranging from hypoxia to complete anoxia, in spring-summer.
107 Anoxia has been found to greatly affect the distribution of nitrogen species in these systems.
108 In order to gain insights into biogeochemical cycling in these poorly investigated water
109 bodies, we selected the Tillari Reservoir for detailed studies. These included measurements of
110 natural abundance of nitrogen and oxygen isotopes in nitrate, and nitrogen and carbon
111 isotopes in POM. These data, first of their kind generated from any Indian freshwater body,
112 facilitate an understanding of biogeochemical processes (especially involving nitrogen) that
113 should be typical of any relatively pristine, tropical, monsoon-affected freshwater body.

114

115 **2.Methods:**

116 **2.1 Site Description:**

117 The Tillari Reservoir is situated in the Dodamarg *taluka* in the Sindhudurg district of
118 Maharashtra (15°76'N, 74°12'E, Fig. 1). Created by damming the Tillari River, the reservoir
119 has a maximum depth of ~50 m and a storage capacity of $0.45 \times 10^9 \text{ m}^3$ (Kurian et al. 2012).
120 The reservoir is located close to the foothills of the Western Ghats, with the drainage basin
121 having evergreen forests (C3 plant type) as well as grasslands (C3 or C4 plant types)
122 (Sukumar et al., 1995). The drainage basin of Tillari has low population density, and so the
123 river water is not much impacted by human activities such as municipal and industrial
124 discharges, and agriculture. This is reflected by high water quality (Shenoy et al., manuscript
125 in preparation). The region receives rainfall averaging around 3000 mm annually, almost
126 entirely between June and September. The evaporation rate in Tillari Reservoir is not known,
127 but for other Indian reservoirs the evaporative loss is reported to average around 0.2 m

128 (Subramanya, 2013) per month. Water from Tillari Reservoir is mainly used for irrigation.
129 Some watershed characteristics of the Tillari Reservoir have been listed in Supplementary
130 Table 1.

131 The Tillari Reservoir is a dimictic water body. Relatively low air temperatures and cool winds
132 descending from the Western Ghats, located immediately to the east of the reservoir, result in
133 convective mixing and well oxygenated conditions in winter. The water column gets
134 thermally stratified in spring and remains so until the strong SWM winds and supply of
135 relatively cold water homogenize the water column again. The water column gets stratified
136 after the SWM. Stratification during spring-summer leads to anoxic condition that is most
137 intense (sulphidic in most years) just before the onset of mixing in June-July. A previous
138 study (Kurian et al, 2012) showed that the occurrence of sulphidic conditions within the
139 euphotic zone supports anoxygenic photosynthesis by brown sulphur bacteria in this
140 reservoir. Methane has been found to accumulate in high concentrations below the
141 thermocline during this period; however, its emissions to the atmosphere are not very high
142 (Narvenkar et al., 2013). Direct human impacts on nutrient inventory of the reservoir are
143 relatively minor, as the basin is located amidst thick forests with low human population
144 density and minimum agricultural activities.

145 **2.2 Sampling and field measurements:**

146 Sampling was conducted at one station located at the deepest part of the reservoir. Water
147 samples from pre-fixed depths were collected with 5-litre Niskin samplers attached to nylon
148 ropes and equipped with reversing thermometers to measure temperature. Subsamples for
149 dissolved oxygen (DO) and hydrogen sulfide (H₂S) were collected carefully avoiding air
150 exchange. Subsamples for nutrients (nitrate and ammonium) were collected in clean 60-ml
151 HDPE bottles and frozen immediately. Subsamples for stable isotopic analyses were collected
152 in 5-litre acid-cleaned plastic carboys and transported to the laboratory within 3-4 hours.

153

154 **2.3 Laboratory analyses:**

155

156 Dissolved O₂ was estimated by the Winkler method (Grasshoff et al., 1983) with a precision
157 of <1 μM. NO₃⁻ and NH₄⁺ were measured using a SKALAR segmented flow analyzer
158 following standard procedures (Grasshoff et al., 1983) with a precision of <0.1 μM.
159 Dissolved H₂S concentration was determined colorimetrically (Cline, 1969).

160

161 **2.4 Isotopic analyses :**

162

163 Sampling for isotopic analyses of POM commenced in March 2010 and continued on a
164 monthly basis till 2012. From 2012 to 2015 samples were collected on a seasonal basis.
165 Samples for nitrate isotopic measurements were collected from 2011. The facility for nitrate
166 isotope analysis was created in 2014 and samples from 2014 and 2015 were analysed
167 immediately for natural abundance of N and O isotopes. Samples from 2011 and 2012 were
168 also analysed on a selective basis. Samples (upto 3l) for isotopic analyses of POM and DIN
169 (dissolved inorganic nitrogen i.e. NO₃⁻ and NH₄⁺) were filtered through precombusted (450° C
170 for 4 hours) 47mm GF/F filters (pore size = 0.7 μm). The filtrate was used for DIN isotopic
171 measurements and the filter papers were placed in petriplates and frozen immediately.

172

173 **2.4.1 Analyses of δ¹⁵N and δ¹⁸O of NO₃⁻:**

174 Samples for isotopic analysis of nitrate were preserved in two ways. While samples collected
175 in 2011 and 2012 were acidified with HCl to pH 2.5, those taken in 2014 and 2015 were
176 frozen immediately and analysed within a week. Prior to the isotopic analyses, nitrate and
177 nitrite concentrations were measured colorimetrically. Isotopic analyses of nitrogen and
178 oxygen in NO₃⁻ were carried out following the “chemical method” (McIlvin and Altabet,
179 2005) involving reduction of NO₃⁻ to NO₂⁻ by cadmium and further reduction to N₂O by

180 sodium azide in an acetic acid buffer. The resulting N_2O gas in the headspace was purged into
181 a GasBench II (Thermo Finnigan) and analysed in a Delta V isotope ratio mass spectrometer.
182 Nitrite concentration was insignificant in most of the samples; sulphamic acid was added in a
183 few samples that contained nitrite in concentrations exceeding $0.1 \mu M$. Working standards
184 were prepared in low-nutrient surface seawater (LNSW) collected from the Arabian Sea.
185 Calibration was done using international nitrate isotope standards USGS-32, USGS-34 and
186 USGS-35. For further quality assurance, an internal potassium nitrate standard (spanning the
187 range of nitrate concentration in the samples) was run with each batch of samples.
188 Magnesium oxide (MgO, Fisher; precombusted for 4 hours at $450^\circ C$) was added to each
189 sample to raise the pH close to 9 which was followed by addition of cadmium. We used
190 cadmium powder (Alfa Aesar, -325 mesh, 99.5%) instead of spongy cadmium as mentioned
191 in McIlvin and Altabet (2005). Each vial was wrapped in aluminium foil and placed on a
192 horizontal shaker at low speed for 17 hours. After the stipulated time, samples were removed
193 from the shaker, centrifuged and decanted into clean vials. The nitrite concentrations in the
194 decanted samples were measured to check the extent of reduction.

195 Sodium azide (2M solution) and 20% acetic acid were mixed in 1:1 proportion (by volume)
196 to yield the azide-acetic acid buffer (A-AA buffer) solution. In 20 ml crimp vials, samples
197 and standards were diluted with LNSW for a final concentration of 20 nmoles and a final
198 volume of 15 ml. Two international nitrite standards (N23 and N20) were added in this step to
199 check the efficiency of N_2O production by the buffer. After addition of the A-AA buffer, the
200 vials were allowed to stand for 1 hour and then the reaction was stopped by adding 0.5ml of
201 10M NaOH.

202 The “chemical” method yielded a very low blank ($\sim 0.5 \mu M$) and worked well for the low
203 concentration samples. The international standards were run before and after each batch of
204 samples, while the internal nitrate standards were run after every 5 samples. Analytical

205 precision (one standard deviation) was better than 0.3‰ for $\delta^{15}\text{N}$ and better than 0.7‰ for
206 $\delta^{18}\text{O}$. Results are expressed in δ notation ($\delta^{15}\text{N}$ and $\delta^{18}\text{O}$), as per mil (‰) deviation from
207 atmospheric nitrogen and Vienna Standard Mean Ocean Water (VSMOW), respectively.

208 **2.4.2 Analyses of $\delta^{15}\text{N}$ of NH_4^+ :**

209 Samples for measurements of $\delta^{15}\text{N}$ - NH_4^+ was collected during May 2012 from the anaerobic
210 hypolimnetic waters. The $\delta^{15}\text{N}$ of NH_4^+ was measured by the “ammonia diffusion” method
211 (Holmes et al., 1998). Briefly, 500 ml of sample was collected in duplicates to which 1.5g of
212 MgO was added to elevate the pH. The diffused NH_4^+ was trapped onto acidified glass-fiber
213 filter sealed between two porous Teflon membranes. The sample bottles were kept in an
214 incubator-shaker (20°C, 80 rpm) for two weeks for complete diffusion of NH_4^+ . After two
215 weeks, the GF filters were removed from each sample, dried in a NH_4^+ -free environment,
216 packed into tin cups and immediately analysed using CF-EA-IRMS. Results were corrected
217 for blank, percent recovery and fractionation. Analytical precision was better than 0.6‰.

218 **2.4.3 Analyses of $\delta^{13}\text{C}$ and $\delta^{15}\text{N}$ of POM and surface sediment:**

219 The analyses of $\delta^{13}\text{C}$ and $\delta^{15}\text{N}$ of POM were usually conducted within 1-2 months of
220 collection. The frozen filters were acid-fumed with 36% HCl to eliminate carbonates and air
221 dried in a clean laminar flow. Two aliquots (each of 12 mm diameter) were sub-sectioned
222 from each filter and packed into tin cups for analysis. Detailed methodology is given in Maya
223 et al. (2011). The $\delta^{13}\text{C}$ and $\delta^{15}\text{N}$ of POM along with particulate C and N contents were
224 analyzed in the same sample using a stable isotope ratio mass spectrometer (Thermo Finnigan
225 Delta V) connected to an elemental analyser (EURO3000 Eurovector). Results are expressed
226 as per mil (‰) deviation with respect to PDB (Pee Dee Belemnite) for $\delta^{13}\text{C}$ and atmospheric
227 nitrogen for $\delta^{15}\text{N}$. Analytical precision was better than $\pm 0.2\text{‰}$ as determined from repeated
228 measurements (after every 5 samples) of a working standard, ϵ -Amino-n-Caproic Acid

229 (ACA) having $\delta^{13}\text{C} = -25.3\text{‰}$ and $\delta^{15}\text{N} = 4.6\text{‰}$, and a laboratory sediment standard having
230 $\delta^{13}\text{C} = -21\text{‰}$ and $\delta^{15}\text{N} = 7.5\text{‰}$.

231 Surface sediment collected from the reservoir during the May 2012 field trip was analysed on
232 only one occasion to investigate its role as an ammonium source. The freeze-dried,
233 homogenized sample was analyzed following similar protocol.

234

235 **3.Results**

236 **3.1 Water column observations**

237 Based on the vertical temperature distribution it appears that the reservoir gets vertically
238 mixed through convective overturning in winter (December to February, with the exact
239 duration of mixing depending upon meteorological conditions prevailing in a given year). In
240 spring stratification sets in and is the most intense from April to June/July (with a surface-to-
241 bottom temperature difference of 7-8°C). The water column is again homogenized following
242 SWM induced mixing and flow of relatively cold water, followed by weaker stratification in
243 autumn/early winter. A detailed discussion on the physico-chemical parameters is provided in
244 Shenoy et al. (manuscript under preparation).

245 The epilimnion was always oxic. During the stratification periods, the DO concentrations
246 dropped rapidly within the thermocline. The water column became well-oxygenated
247 following the onset of the southwest monsoon. H_2S was detected below 20 m during the
248 period of intense stratification (Kurian et al., 2012), with the highest concentration recorded
249 being 9.88 μM . The occurrence of H_2S was accompanied by the appearance of CH_4 and NH_4^+ .
250 Upto 160 μM of CH_4 and 30 μM of NH_4^+ were observed in the anoxic bottom waters during
251 peak summer (Narvenkar et al., 2013) [\(Fig. 6\)](#).

252 A thorough analysis of nutrient dynamics in Tillari Reservoir is provided by Naik et al.
253 (manuscript under preparation). Here we provide a brief description of nitrate profiles during
254 the study period. Surface water nitrate concentrations were typically low throughout the year
255 ranging from below detection limit to 0.7 μM . However, the surface nitrate concentrations
256 were as high as $\sim 10 \mu\text{M}$ (Fig. 3a) during the SW Monsoon. Nitrate concentrations gradually
257 increased below the epilimnion during the period of weak stratification. However, with the
258 depletion of DO, nitrate concentrations in the hypolimnion decreased from 3.6 μM (at 20m)
259 to 0.3 μM (at 35m), indicating N-loss. Reoxygenation of hypolimnion during the SW
260 monsoon was accompanied by increase in nitrate concentrations (5-10 μM).

261 **3.2 Isotopic composition of nitrate and ammonium**

262 Large variations in the isotopic composition of nitrate and ammonium were observed in space
263 and time. Isotopic composition of nitrate in the epilimnion could not be measured on several
264 occasions due to low concentrations. However, when the measurements could be made it was
265 observed that the $\delta^{15}\text{N}$ and $\delta^{18}\text{O}$ values of epilimnetic (0-10 m) NO_3^- were high ($\delta^{15}\text{N} = 8$ -
266 25‰ , $\delta^{18}\text{O} = 24$ - 29‰) (Fig 3b) during the summer stratification presumably due to
267 autotrophic assimilation whereas relatively lower values ($\delta^{15}\text{N} = 5$ - 8‰ , $\delta^{18}\text{O} = 12$ - 15‰) were
268 observed during the monsoon mixing events. Increasing $\delta^{15}\text{N}$ and $\delta^{18}\text{O}$ of NO_3^- , coupled to
269 decreasing $[\text{NO}_3^-]$, were also observed in the suboxic hypolimnion during April and May,
270 when the water column was strongly stratified. The highest $\delta^{15}\text{N}$ values observed were 27.7‰
271 (in 2014) and 22.4‰ (in 2012) while the corresponding highest $\delta^{18}\text{O}$ values were 29.5‰ and
272 28.8‰ , respectively.

273 The water column remains weakly stratified for a large part of the year, usually from October
274 to March. A trend of increasing concentrations of isotopically light ($\delta^{15}\text{N} = 2$ - 8‰ and $\delta^{18}\text{O} =$
275 5 - 8‰) nitrate was observed in the hypolimnion along with gradually decreasing levels of

276 oxygen and ammonium implying the occurrence of nitrification. As the stratification
277 intensified, this phenomenon was restricted only to the metalimnion. After nitrate was
278 exhausted, high ammonium build up was observed in the bottom waters. In May 2012, NH_4^+
279 concentrations increased from 0.6 μM at 20m to nearly 12 μM at 40m with a corresponding
280 decrease in $\delta^{15}\text{N-NH}_4^+$ from 2.6‰ at 20m to 1.3‰ at 40m (Fig. 5a).

281 Elevated nitrate concentrations occur throughout the water column during the SW monsoon.
282 The $\delta^{15}\text{N}$ and $\delta^{18}\text{O}$ of NO_3^- showed little vertical variations at this time. However, interannual
283 variability was seen in the $\delta^{15}\text{N}$ of nitrate ($3.94 \pm 2.4\%$ in 2011, $11.38 \pm 1.6\%$ in 2014, and
284 $5.47 \pm 1.8\%$ in 2015), the cause of which will be examined. By contrast, the $\delta^{18}\text{O-NO}_3^-$ values
285 were relatively less variable ($13.01 \pm 4.8\%$ in 2011, $15.41 \pm 2.3\%$ in 2014, and $12.46 \pm 4.9\%$ in
286 2015).

287 3.3 Isotopic and elemental composition of suspended particulate organic 288 matter

289 The suspended particulate organic matter in the Tillari Reservoir showed distinct seasonal
290 and depth-wise variations in its isotopic and elemental compositions (Fig. 2). Primary
291 productivity in the epilimnion led to higher $\delta^{15}\text{N}$ (2‰ to 6‰) and $\delta^{13}\text{C}$ (-28% to -26%) in
292 POM and higher POC (35-60 μM) and PON (4-6 μM) contents as compared to the bottom
293 water. The molar C/N ratios in the surface waters ranged between 7 and 10. Depleted $\delta^{15}\text{N}$
294 ($\sim -1.4\%$) in the epilimnion was observed during the early stratification period (February and
295 March). As the stratification intensified, the $\delta^{15}\text{N}$ and $\delta^{13}\text{C}$ of the epilimnetic POM became
296 heavier, presumably reflecting a gradual enrichment of heavier isotopes in the dissolved
297 inorganic N and C pools. Both $\delta^{15}\text{N}$ and $\delta^{13}\text{C}$ decreased with depth with the lowest values
298 occurring in the anoxic bottom water during peak stratification period. The C/N values in
299 these waters were in the range of 4-7. In terms of seasonal variability, $\delta^{13}\text{C}$ values of POM

300 were lower during monsoon mixing and became more enriched as the stratification
301 intensified. The $\delta^{15}\text{N}$ values, however, did not depict any distinct seasonal pattern. High POC
302 (upto 80 μM) and PON (upto 9 μM) along with high C/N (>10) were recorded during the
303 monsoon season apparently reflecting allochthonous inputs.

304 **4. Discussion:**

305 **4.1 Epilimnetic processes:**

306 Nitrate concentrations in surface waters of the Tillari Reservoir varied from below detection
307 limit during the premonsoon period to 10.7 μM during the SW monsoon. The $\delta^{18}\text{O}$ and $\delta^{15}\text{N}$
308 values of nitrate in the epilimnion were high, a signature of assimilation: phytoplankton
309 prefer nitrate containing ^{14}N and ^{16}O leaving residual nitrate enriched with $\delta^{15}\text{N}$ and $\delta^{18}\text{O}$
310 (Casciotti et al., 2002). We examined the slopes of the $\delta^{18}\text{O}$ vs. $\delta^{15}\text{N}$ regression in the surface
311 water. While a 1:1 line would represent assimilation of epilimnetic nitrate, a steeper slope
312 would imply assimilation along with the regeneration of nitrate via nitrification (Wankel et
313 al., 2007). We observed a nearly 1:1 trend for most of the surface water samples during the
314 summer stratification implying that assimilation exerts the major control on surface NO_3^-
315 isotopic composition (Supplementary Fig. 1).

316 The isotopic composition of the DIN source exerts the key control on the $\delta^{15}\text{N}$ of POM
317 (Altabet, 2006). The epilimnetic POM in the Tillari Reservoir is expected to have $\delta^{15}\text{N}$ less
318 than or equal to the $\delta^{15}\text{N}$ - NO_3^- . Indeed, the $\delta^{15}\text{N}$ -POM was always lower than the $\delta^{15}\text{N}$ of the
319 source nitrate (Fig. 3b). The range of $\delta^{13}\text{C}$ values of surface-water POM (-32 to -26‰) was
320 typical of lacustrine autochthonous organic matter (-42 to -24‰, Kendall et al., 2001 and
321 references therein). As the summer progressed, productivity increased resulting in increased
322 CO_2 uptake and elevated $\delta^{13}\text{C}$ -POM. During photosynthesis, phytoplankton preferentially

323 uptake ^{12}C leaving the DIC (dissolved inorganic carbon) pool enriched in ^{13}C . However, when
324 dissolved C is scarce and/or growth rate is high, the phytoplankton would consume the
325 available DIC with reduced or no isotopic discrimination. As the summer progressed at the
326 study location, increased water temperature and low dissolved inorganic nutrient and DIC
327 concentrations would cause the phytoplankton to express reduced isotopic discrimination.
328 This would result in enriched $\delta^{13}\text{C}$ of POM. Similar enrichment of $\delta^{13}\text{C}$ -POM during periods
329 of high productivity have also been observed in other lakes, for e.g., Lake Lugano (Lehmann
330 et al., 2004) and Lake Wauberg (Gu et al., 2006).

331 In March, when nitrate was close to detection limit, surface $\delta^{15}\text{N}$ -POM was -1.4‰ . The POM
332 resulting from nitrogen fixation by cyanobacteria usually has a $\delta^{15}\text{N}$ of 0 to -2‰ (Carpenter
333 et al., 1997). Zeaxanthin, marker pigment of cyanobacteria, was present in significant
334 concentrations ($305.1 \pm 21 \text{ ng l}^{-1}$) within the epilimnion, whereas Chl-*a* concentration was ~ 1.7
335 $\mu\text{g l}^{-1}$ (S. Kurian, unpublished data). However, measurements of nitrogen fixation rates in the
336 Tillari Reservoir have yielded very low values during summer (unpublished data).
337 Alternatively, the lower $\delta^{15}\text{N}$ values may also result from isotopically light nitrate that is
338 produced in the hypolimnion and diffuses upward into surface waters. Another possible
339 source of isotopically lighter N could be atmospheric deposition, although the magnitude of
340 atmospheric inputs is not expected to be very large during early summer. Further work is
341 required to understand the episodic occurrence of low $\delta^{15}\text{N}$ -POM.

342 **4.2 Biogeochemistry of hypolimnion**

343 **4.2.1 Nitrification:**

344 Stratification in the Tillari Reservoir sets in soon after the decline of the monsoon-fed inflow
345 following which nitrate concentrations increased in oxygenated bottom waters with a
346 concomitant decrease in ammonium concentrations, indicating the occurrence of nitrification.

347 The nitrate concentrations ranged from below detection limit in the upper 10 m to nearly 10
348 μM close to the bottom. Nitrification occurs in two steps: ammonia oxidation to nitrite
349 (performed by ammonia oxidising archaea and bacteria) and nitrite oxidation to nitrate
350 (performed by nitrite oxidising bacteria). Ammonium, the primary N source, undergoes
351 strong fractionation producing isotopically light nitrate (Delwiche and Stein, 1970, Casciotti
352 et al., 2003). The $\delta^{15}\text{N}\text{-NO}_3^-$ values ranged from 2-10‰ and the $\delta^{18}\text{O}\text{-NO}_3^-$ ranged from 5-
353 8‰ during this period. Nitrate accumulation due to atmospheric deposition and microbial
354 nitrification will have distinct $\delta^{18}\text{O}\text{-NO}_3^-$ values. This is because, while the oxygen atoms in
355 atmospheric nitrate are derived from interactions between NO_x and O_3 in the atmosphere,
356 those in nitrate produced by nitrification come from dissolved oxygen and water (Kendall,
357 1998, Finlay et al., 2007). This is well reflected in the $^{15}\text{N}\text{-}^{18}\text{O}$ scatter plot where the $\delta^{18}\text{O}\text{-}$
358 NO_3^- data-points from the epilimnion and hypolimnion form completely distinct clusters in
359 February (Fig 4). As the ammonium pool gets used up, the nitrification rate decreases
360 accompanied by a decrease in the extent of fractionation (Feigin et al., 1974).

361 Ammonium, oxygen and carbon dioxide are the major substrates needed for nitrification
362 (Christofi et al., 1981). While ammonium largely comes from the sediments, oxygen is
363 supplied from aerated surface waters. During the early stratification period, conducive
364 conditions exist for nitrifiers to grow within the hypolimnion. However, as the bottom waters
365 turn increasingly more oxygen-depleted with the intensification of stratification the
366 “ammonium-oxygen chemocline” (Christofi et al., 1981) moves upward in the water column
367 and the metalimnion becomes more suitable for the occurrence of nitrification. In April 2014,
368 $\delta^{18}\text{O}$ declined within the thermocline from 34‰ at 5m to 14‰ at 20m owing to nitrification.
369 Epilimnetic nitrate isotope data are not available for 2012 due to very low nitrate
370 concentrations. However, the $\delta^{18}\text{O}$ declined from 25‰ at 15m to 17‰ at 20m. The $\delta^{15}\text{N}$
371 values in both the years did not show a similar decline, but this is consistent with the results

372 of several other studies (Böttcher et al., 1990; Burns and Kendall, 2002), where the $\delta^{18}\text{O}$ was
373 found to be better suited for source and process identification than $\delta^{15}\text{N}$. It may be noted that
374 this decoupling of $\delta^{15}\text{N}$ and $\delta^{18}\text{O}$ was only observed during the peak stratification period at
375 the thermocline.

376 The $\delta^{15}\text{N}$ and $\delta^{13}\text{C}$ values for the POM were generally low during the nitrification period as
377 also observed in Lake Kinneret (Hadas et al., 2009). The $\delta^{15}\text{N}$ varied from -4‰ to 3‰ while
378 $\delta^{13}\text{C}$ varied from -31‰ to -29‰ . Assimilation of newly nitrified NO_3^- may be a possible
379 contributor to POM as indicated by the low $\delta^{15}\text{N}$ values.

380 **4.2.2 Denitrification:**

381 During the period of strong stratification, the water column loses oxygen below the
382 thermocline, which apparently results in N loss. Along with a decrease in nitrate, there also
383 occurs an increase in NH_4^+ concentration. Dissimilatory nitrate reduction is known to be
384 associated with 1:1 increase in $\delta^{15}\text{N-NO}_3^-$ and $\delta^{18}\text{O-NO}_3^-$ (Granger et al., 2008). Linear
385 regression of $\delta^{18}\text{O}$ versus $\delta^{15}\text{N}$ yielded slope values of 0.95 and 0.85 in 2014 and 2012,
386 respectively. In canonical denitrification, both $\delta^{15}\text{N-NO}_3^-$ and $\delta^{18}\text{O-NO}_3^-$ increase linearly.
387 The enrichment in isotopic value is ~ 1 in marine systems (Casciotti et al., 2002, Sigman et
388 al., 2005, Granger et al., 2008). However, this value is reported to be lower (0.5-0.7) in
389 freshwater systems (Lehmann et al., 2003 and references therein). The reasons for this
390 difference are not fully understood. Also, studies in freshwater systems are sparse as
391 compared to marine systems. In a batch of culture experiments, Granger et al. (2008)
392 observed that nitrate-reducing enzymes play a role in altering the O to N isotopic enrichment,
393 with periplasmic dissimilatory nitrate reductase (Nap) expressing a lower enrichment value
394 (~ 0.62) than the membrane-bound dissimilatory nitrate reductase. Again, there is a lack of
395 data on the isotopic expressions of these enzymes at the ecosystem level. Wenk et al. (2014)

396 attributed the low O:N isotopic effect of ~ 0.89 to chemolithoautotrophic denitrification,
397 rather than heterotrophic denitrification, in the northern basin of Lake Lugano.

398 Our data from the Tillari reservoir indicates the occurrence of denitrification in the suboxic
399 hypolimnion under stratified conditions. However, this process is restricted to a narrow depth
400 range of 10-20 m which limits the number of data points. There may be several factors
401 responsible for the low (< 1) isotopic enrichment factor in the Tillari but our data are not
402 sufficient to identify the exact cause(s).

403 Assuming the N loss was largely through denitrification, an attempt was made to compute the
404 fractionation factor using a Rayleigh “closed-system” model (Lehmann et al., 2003).
405 Although there have been several attempts to compute the nitrogen isotope enrichment
406 factors in marine systems, ground waters and laboratory cultures (Table 1); similar
407 information is relatively scarce from freshwater lakes and reservoirs.

408 The available information on oxygen isotope fractionation is even scarcer. The values of ϵ^{15}
409 and ϵ^{18} computed by us are -8.7‰ and -10.7‰ , respectively. The ϵ^{15} is much lower than
410 those obtained from laboratory cultures (Olleros, 1983; Table 1) as well as open-ocean OMZs
411 (Brandes et al., 1998, Voss et al., 2001; Table 1) although it is close to the ϵ^{15} reported from
412 the eutrophic Lake Lugano. Factors controlling denitrification rates in aquatic systems
413 include temperature, availability of nitrate and organic carbon, oxygen concentration and type
414 of bacterium involved (Seitzinger et al., 1988, Bottcher et al., 1990, and references therein).
415 Sedimentary denitrification is known to incur isotope effect (ϵ^{15}) of $\sim 0\text{‰}$ due to almost
416 complete exhaustion of nitrate. The dissolved nitrate concentrations in the Tillari Reservoir
417 are quite low with the highest values being in the range of 10-12 μM (see Results). The
418 hypolimnetic nitrate concentrations were even lower ($< 5 \mu\text{M}$) during periods of anoxia. Low
419 nitrate availability and sedimentary N-loss may exert major controls on the low ϵ^{15} observed
420 in the Tillari Reservoir.

421 Denitrification strongly discriminates among the two N isotopes, leaving behind ^{15}N -enriched
422 in the residual NO_3^- . POM produced by assimilation of this nitrate will also be enriched in
423 ^{15}N . However, lower $\delta^{15}\text{N}$ -PON at these depths implies that NH_4^+ was the preferred DIN
424 source. For instance, observations in April 2012 showed that denitrification was active below
425 30m and associated with ammonium build-up, there was nearly a 4‰ depletion in $\delta^{15}\text{N}$ -PON
426 from 2.5‰ (at 30m) to -2.3‰ (at 40m).

427 **4.2.3 Ammonification:**

428 The isotopic composition of ammonium should reflect that of the sedimentary organic matter
429 being degraded. In Lake Kinneret (Israel), $\delta^{15}\text{N}$ - NH_4^+ values in the hypolimnion during
430 stratified conditions ranged from 12 to 17 ‰ reflecting the high $\delta^{15}\text{N}$ of the sedimentary OM
431 ($\delta^{15}\text{N} = 10\text{‰}$) (Hadas et al., 2009). In Lake Bled (NW Slovenia), mean $\delta^{15}\text{N}$ - NH_4^+ value of
432 3.8‰ was similar to that of sedimentary OM ($\delta^{15}\text{N} = 4.5\text{‰}$) (Bratkic et al., 2012). Likewise,
433 the sedimentary OM in the Tillari Reservoir had a $\delta^{15}\text{N}$ of 2.96‰ similar to the $\delta^{15}\text{N}$ - NH_4^+
434 (1.3-2.6‰) thus establishing remineralization of sedimentary OM as the principal NH_4^+
435 source.

436 A negative linear relationship between $\delta^{15}\text{N}$ -PON and $\ln[\text{NH}_4^+]$ was observed (Fig. 5b) which
437 further indicated uptake of NH_4^+ . Although this relation was mainly determined by the low
438 $[\text{NH}_4^+]$ and high $\delta^{15}\text{N}$ -PON observed at the top of the hypolimnion (20m), it is important to
439 include this datapoint to highlight the rapid decline of $\delta^{15}\text{N}$ -PON over a short depth range.

440 The fractionation factor (ϵ) calculated from the slope was -2.4‰. The fractionation factor for
441 ammonium assimilation has been estimated in several field studies (Cifuentes et al., 1988;
442 Bratkic et al 2012) as well as in lab cultures with different organisms (green algae, marine
443 bacteria, etc) (Wada & Hattori, 1978, Wada 1980, Hoch et al 1992). However, such studies in
444 freshwater lakes and reservoirs are scarce. Bratkic et al. (2012) computed fractionation

445 factors of -0.8‰ and -1.4‰ for mean ammonium concentrations of $4.7\ \mu\text{M}$ and $3.3\ \mu\text{M}$
446 respectively in Lake Bled. Hoch et al. (1992) reported fractionation factor for assimilation by
447 *Vibrio harveyi*, a marine bacterium, to be between -4‰ and -27‰ for ammonium
448 concentrations ranging from 23 to $180\ \mu\text{M}$. The fractionation factor is expected to approach
449 0‰ for decreased concentrations of ammonium. For the low to moderate ammonium
450 concentrations recorded (maximum $\sim 12\ \mu\text{M}$ in Figure 5) the fractionation factor computed by
451 us compares well with previously reported values.

452 4.2.4 Sulphate reduction and evidence for chemosynthesis:

453 As the summer intensified and oxidized nitrogen was fully utilized, facultative bacteria
454 apparently began to utilize sulphate as an electron acceptor as indicated by the accumulation
455 of H_2S . Mass dependent fractionation during microbial degradation of organic matter with
456 sulphate as an electron acceptor would the residual organic matter enriched in ^{13}C and ^{15}N .
457 However, following the appearance of H_2S , both $\delta^{13}\text{C}\text{-POC}$ and $\delta^{15}\text{N}\text{-PON}$ became more
458 depleted. The $\delta^{15}\text{N}$ values varied between -8‰ and -5‰ and $\delta^{13}\text{C}$ values ranged from -37‰
459 to -32‰ between 30 and 40m depths. The accumulation of H_2S was also accompanied by
460 significant build-up of CH_4 ($20\text{-}150\ \mu\text{M}$) and NH_4^+ ($1\text{-}20\ \mu\text{M}$) (Naik et al., manuscript in
461 prep.). Increases in POC and PON contents were also observed: from $28\ \mu\text{M}$ to $60\ \mu\text{M}$ for
462 POC and from 4.7 to $8\ \mu\text{M}$ for PON. Bacterial assimilation of ammonium can explain the
463 isotopically light nitrogen, but utilization of biogenic methane is known to lead to extremely
464 low $\delta^{13}\text{C}$ values (between -65‰ and -50‰ ; Whiticar et al., 1986). In our study, the most
465 depleted $\delta^{13}\text{C}\text{-POC}$ value of -37.8‰ was associated with the highest methane concentration
466 of $156\ \mu\text{M}$. Interestingly, in a study carried out in the waters of Lake Baikal in Siberia, very
467 negative $\delta^{13}\text{C}\text{-DIC}$ values (-28.9 to -35.6‰) were inferred to be derived from methane
468 oxidation while the $\delta^{13}\text{C}\text{-POC}$ values (-31.7 to -33.5‰) were typical of lacustrine organic

469 matter (Prokopenko and Williams 2005). The authors explained this lack of correlation
470 between the two C pools by a possible time lag between the peak methane oxidation and peak
471 productivity. Low $\delta^{13}\text{C}$ -POC ($\sim -37\text{‰}$) in Lake Kinneret was attributed to chemosynthetic C
472 fixation using depleted $\delta^{13}\text{C}$ -DIC derived from methane oxidation (Hadas et al. 2009). It is
473 important to understand the fate of methane in freshwater systems as they are believed to be
474 significant contributors to atmospheric methane emissions (Bastviken et al., 2004). The
475 POM isotopic data of the Tillari Reservoir provides evidence for intense microbial
476 chemosynthesis using sulphide, ammonia and methane as energy donors.

477 **4.3 Monsoon mixing in Tillari Reservoir:**

478 The reservoir gets vertically mixed during the months of July, August and September due to a
479 combination of lower atmospheric temperature, strong winds and inflow of relatively cold
480 water during the southwest monsoon. Nitrate concentrations are moderately high throughout
481 the water column, although variable from one year to another. The mean water-column nitrate
482 concentration were $7.26 \pm 2.8 \mu\text{M}$ ($n = 10$) in 2011, $9.29 \pm 0.8 \mu\text{M}$ ($n = 10$) in 2014, and
483 $8.13 \pm 4.7 \mu\text{M}$ ($n = 9$) in 2015. The isotopic composition of nitrate also showed inter-annual
484 variability. While the water column was uniformly nitrate-replete in 2014, the epilimnetic (0-
485 5 m) nitrate concentrations in 2011 and 2015 were markedly lower than those at deeper
486 depths (Fig.7), except at two deepest samples in 2015. This may indicate nitrate uptake by
487 phytoplankton. However, considering its high concentration in rainwater, ammonium is
488 expected to compete with nitrate for phytoplankton uptake. Moreover, the $\delta^{15}\text{N}$ of nitrate in
489 the epilimnion was lower in 2011 and 2015 than in 2014. In fact, elevated values of $\delta^{15}\text{N}$ -
490 NO_3^- ($>8\text{‰}$) occurred throughout the water column in 2014 when the nitrate concentration
491 was also generally higher as compared to the other two years. To investigate the cause of this
492 variability, water samples from six upstream stations along the Tillari River along with a

493 rainwater sample at the main station were collected in 2015. The nitrate concentrations
494 ranged from 1.8 μM at the most upstream station to 9.4 μM close to our main sampling site.
495 The ranges of $\delta^{15}\text{N}$ and $\delta^{18}\text{O}$ of NO_3^- at these stations were 0.4-6.8‰ and 11-27‰,
496 respectively. The rainwater sample had a nitrate content of 13.89 μM (ammonium = 24.4 μM)
497 and yielded $\delta^{15}\text{N}$ and $\delta^{18}\text{O}$ values of -2.9‰ and 88.7‰, respectively. Nitrate in wet
498 deposition is usually characterised by high $\delta^{18}\text{O}$ ($> 60\text{‰}$) (Kendall et al., 2007; Thibodeau et
499 al., 2013) and low $\delta^{15}\text{N}$ (-10 to $+5 \text{‰}$) (Heaton et al., 2004) values. Unfortunately, the
500 concentration and isotopic composition of these end members (river runoff and atmospheric
501 deposition) do not explain the data from the Tillari especially from the 2015. Based on the
502 high concentration of nitrate in rainwater, it is tempting to suggest that it could be an
503 important source, but the isotopic data show a mismatch. The $\delta^{13}\text{C}$ -POC values in the
504 epilimnion decreased to nearly -30‰ presumably due to a combination of lower primary
505 productivity and inputs of organic matter through runoff. Even though the latter was not
506 measured POC derived from land vegetation is expected to be isotopically light. The POM
507 data show the ingress of a nearly 30m thick parcel of water from the Tillari River into the
508 reservoir. This ingress is apparent below 5m depth by distinct $\delta^{13}\text{C}$ and $\delta^{15}\text{N}$ of POM. The
509 $\delta^{13}\text{C}$ -POC increases from -30.9‰ ($\pm 0.1\text{‰}$) in the upper 5m to -25.4‰ ($\pm 1\text{‰}$) between 5m
510 and 40m. Below 40m, the mean $\delta^{13}\text{C}$ -POC was -26.5‰ ($\pm 1.7\text{‰}$). The mean $\delta^{15}\text{N}$ of the
511 intermediate water parcel was $5.97 \pm 2\text{‰}$, as compared to $5.49 \pm 3\text{‰}$ in the bottom waters and
512 $3.96 \pm 2\text{‰}$ in the upper 5m. The isotopic data correspond well with the ancillary chemical
513 parameters, in that the water parcel had a distinct thermal signature (cooler by nearly 2°C). It
514 also possessed higher levels of nitrate and lower levels of DO and chlorophyll-*a*.

515 Thus, looking solely at the high nitrate concentrations in the water column, atmospheric wet
516 deposition may be a major nitrate source to the water column during the monsoon season.
517 However, this inference is based on a single measurement where the isotopic composition is

518 also different. Moreover, the river water is also rain-fed and it is not clear why its isotopic
519 composition is much lower at the most upstream station. At the same time, the isotopic
520 composition of POM indicates influence of the upstream waters. Variable inputs from the
521 atmosphere and by river runoff to the DIN pool probably account for the interannual
522 variability, but more studies are needed to identify and quantify these contributions in detail.

523 **5. Summary and Conclusions:**

524 Using stable isotopes of nitrate, ammonium and particulate organic matter, we have been able
525 to identify distinct water column conditions and transformation processes of reactive nitrogen
526 in the Tillari Reservoir. The reservoir gets vertically mixed during the southwest monsoon
527 season as well as in winter; the water column remained stratified during other parts of the
528 year. The most intense stratification occurs during summer just before the monsoon onset.
529 Relative importance of microbial processes such as nitrification, denitrification,
530 ammonification and sulphate reduction in the water column varied depending on intensity of
531 stratification and associated DO levels in the hypolimnion. These processes produced unique
532 isotopic signatures in the dissolved and particulate matter. Our results suggest the occurrence
533 of microbial chemosynthesis using methane and ammonium as primary C- and N- sources,
534 producing organic matter in the anoxic bottom waters that is highly depleted in ^{13}C and ^{15}N
535 content. The thermocline in the Tillari Reservoir has been known to harbour photoautotrophic
536 sulphur bacteria during peak stratification periods (Kurian et al., 2012). We also found strong
537 signatures of nitrification within this zone during summer stratification. Autochthonous
538 production was the principal source of organic matter in the epilimnion which was well-
539 oxygenated at all times, although productivity was significantly lower during the monsoon
540 period due to light-limited conditions. Nitrate was the preferred DIN source in the
541 epilimnion. When nitrate loss occurred in the hypolimnion, the preferred DIN species

542 switched from nitrate to ammonium. Isotopic measurement of precipitation and upstream
543 river samples during one seasonal sampling provided some insight into sources of nitrogen,
544 but the observed inter-annual variability could not be explained. Overall, solar intensity,
545 water depth and redox conditions appear to be the major factors controlling biogeochemical
546 cycling in this pristine reservoir.

547 **Acknowledgements:**

548 We thank the Director, CSIR-NIO for providing necessary support for this work and the
549 management body of the Tillari reservoir for permission to carry out this study. This research
550 was carried out as a part of INDIAS IDEA project funded by the Council of Scientific &
551 Industrial Research (CSIR). The authors wish to thank Mark Altabet and Laura Bristow for
552 sharing their expertise. We thank Prof. Sugata Hazra and the School of Oceanographic
553 Studies, Jadavpur University for their support and encouragement. Puja Satardekar is
554 acknowledged for analyzing the nutrient samples. Sujal Bhandodkar (DTP section, CSIR-NIO)
555 is thanked for her creative inputs. P. Bardhan thanks CSIR for the award of Senior Research
556 Fellowship. The authors are also grateful to Ms. Maya MV for her initial assistance in
557 isotopic analyses and to Mr. H. Dalvi, Mr. A. Methar, Mr. Jonathan and Mr. Sumant for their
558 help during field work. This is NIO Contribution no. XXXX.

559 **References**

560 Altabet, M. A.: Variations in nitrogen isotopic composition between sinking and suspended
561 particles: Implications for nitrogen cycling and particle transformation in the open ocean,
562 *Deep-Sea Res.*, 35, 535–554, 1988.

563
564 Altabet, M. A.: Isotopic tracers of the marine nitrogen cycle, in: *Marine organic matter:
565 Chemical and biological markers*, edited by: Volkman, J., *The handbook of environmental
566 chemistry*, Springer-Verlag, 251–293, 2006.

567
568 Bastviken, D., Cole, J. J., Pace, M., and Tranvik, L.: Methane emissions from lakes:
569 Dependence of lake characteristics, two regional assessments, and a global estimate, *Glob.
570 Biogeochem. Cy.*, 18:GB4009, doi: 10.1029/2004GB002238, 2004.

571

572 Böttcher, J., Strebel, O., Voerkelius, S., and Schmidt, H.-L.: Using isotope fractionation of
573 nitrate-nitrogen and nitrate-oxygen for evaluation of microbial denitrification in a sandy
574 aquifer, *J. Hydrol.*, 114, 413–424, doi: 10.1016/0022-1694(90)90068-9, 1990.
575

576 Brandes, J. A., Devol, A. H., Yoshinari, T., Jayakumar, D. A., and Naqvi, S. W. A.: Isotopic
577 composition of nitrate in the central Arabian Sea and eastern tropical North Pacific: A tracer
578 for mixing and nitrogen cycles, *Limnol. Oceanogr.*, 43, 1680–1689, doi:
579 10.4319/lo.1998.43.7.1680, 1998.
580

581 Bratkic, A., Sturm, M., Faganeli, J., and Ogrinc, N.: Semi-annual carbon and nitrogen isotope
582 variations in the water column of Lake Bled, NW Slovenia, *Biogeosciences*, 9, 1–11. doi:
583 10.5194/bg-9-1-2012, 2012.
584

585 Burns, D. A. and Kendall, C.: Analysis of ¹⁵N and ¹⁸O sources in runoff at two watersheds in
586 the Catskill Mountains of New York, *Water Resour. Res.*, 38, 1051, doi: 10.1029/
587 2001WR000292, 2002.
588

589 Carpenter, E. J., Harvey, H. R., Fry, B., and Capone, D. G.: Biogeochemical tracers of the
590 marine cyanobacterium *Trichodesmium*, *Deep-Sea Res. Pt. I*, 44, 27–38, 1997.
591

592 Casciotti, K. L., Sigman, D. M., Galanter Hastings, M., Bohlke, J. K., and Hilkert, A.:
593 Measurement of the oxygen isotopic composition of nitrate in seawater and freshwater using
594 the denitrifier method, *Anal. Chem.*, 74, 4905–4912, 2002.
595 Casciotti, K. L., Sigman, D. M., and Ward, B. B.: Linking diversity and stable isotope
596 fractionation in ammonia-oxidizing bacteria, *Geomicrobiol. J.*, 20, 335–353, 2003.
597

598 Chen, F. J. and Jia, G. D.: Spatial and seasonal variations in $\delta^{13}\text{C}$ and $\delta^{15}\text{N}$ of particulate
599 organic matter in a dam-controlled subtropical river, *River Res. Appl.*, 25, 1169–1176, doi:
600 10.1002/rra.1225, 2009.
601

602 Chen, F., Jia, G., and Chen, J.: Nitrate sources and watershed denitrification inferred from
603 dual isotopes in the Beijiang River, South China, *Biogeochemistry*, 94, 163–174, doi:
604 10.1007/s10533-009-9316-x, 2009.
605

606 Chen, Z.X., Yu, L., Liu, W.G., Lam, M.H.W., Liu, G.J., and Yin, X. B.: Nitrogen and oxygen
607 isotopic compositions of water-soluble nitrate in Taihu Lake water system, China: implication
608 for nitrate sources and biogeochemical process, *Environ Earth Sci.*, 1, 217–223, 2014.
609

610 Christofi, N., Preston, T. and Stewart, W.D.P.: Endogenous nitrate production in an
611 experimental enclosure during summer stratification, *Water research*, 15(3), 343-349, doi:
612 10.1016/0043-1354(81)90039-7, 1981.
613

614 Cifuentes, L. A., Sharp, J. H., and Fogel, M. L.: Stable carbon and nitrogen isotope
615 biogeochemistry in the Delaware Estuary, *Limnol. Oceanogr.*, 33, 1102–1115, 1988.
616

617 Cline, J.D.: Spectrophotometric determination of hydrogen sulfide in natural waters, *Limnol.*
618 *Oceanogr.*, 14, 454–458, 1969.
619

620 Dähnke, K., and Thamdrup, B.: Nitrogen isotope dynamics and fractionation during
621 sedimentary denitrification in Boknis Eck, Baltic Sea, *Biogeosciences*, 10, 3079–3088. doi:
622 10.5194/bg-10-3079-2013, 2013.

623

624 Delwiche, C. C., and Stein, P. L.: Nitrogen isotope fractionation in soil and microbial
625 reactions, *Environ. Sci. Tech.*, 4, 929-935, 1970.

626

627 Feigin, A., Shearer, G., Kohl, D.H. and Commaner, B.: The amount and nitrogen -15 content
628 of nitrate in soil profiles from two central Illinois fields in a corn-soybean rotation, *Soil Sci.*
629 *Soc. Amer. Proc.*, 38, 465–471, 1974.

630

631 Finlay, J. C., Sterner, R. W., and Kumar, S.: Isotopic evidence for in-lake production of
632 accumulating nitrate in Lake Superior, *Ecol. Appl.*, 17, 2323–2332, doi: 10.1890/07-0245.1,
633 2007.

634

635 Granger, J., Sigman, D. M., Lehmann, M. F., and Tortell, P. D.: Nitrogen and oxygen isotope
636 fractionation during dissimilatory nitrate reduction by denitrifying bacteria, *Limnol.*
637 *Oceanogr.*, 53, 2533–2545, 2008.

638

639 Grasshoff, K., Ehrhardt, M., and Kremling, K.: *Methods of seawater analysis*, 2 Edn., 419
640 pp., Weinheim: Verlag Chemie., 1983.

641 Gu, B., Chapman, A. D., and Schelske, C. L.: Factors controlling seasonal variations in stable
642 isotope composition of particulate organic matter in a soft water eutrophic lake, *Limnol.*
643 *Oceanogr.*, 51, 2837-2848, 2006.

644

645 Hadas, O., Altabet, M. A., and Agnihitori, R.: Seasonally varying nitrogen isotope
646 biogeochemistry of particulate organic matter in lake Kinneret, Israel, *Limnol. Oceanogr.*, 54,
647 75–85, 2009.

648

649 Heaton, T. H. E.: Isotopic studies of nitrogen pollution in the hydrosphere and atmosphere: A
650 review, *Chem. Geol.*, 59, 87-102, 1986.

651

652 Hoch, M. P., Fogel, M. L., and Kirchman, D. L.: Isotope fractionation associated with
653 ammonium uptake by a marine bacterium, *Limnol. Oceanogr.*, 37, 1447-1459, 1992.

654

655 Holmes, R. M., McClelland, J. W., Sigman, D. M., Fry, B., and Peterson, B. J.: Measuring
656 $^{15}\text{N-NH}_4^+$ in marine, estuarine and fresh waters: an adaptation of the ammonia diffusion
657 method for samples with low ammonium concentrations, *Mar. Chem.*, 60, 235–243,
658 doi: 10.1016/S0304-4203(97)00099-6, 1998.

659

660 Hu, H., Bourbonnais, A., Larkum, J., Bange, H. W., and Altabet, M. A.: Nitrogen cycling in
661 shallow low oxygen coastal waters off Peru from nitrite and nitrate nitrogen and oxygen
662 isotopes. *Biogeosciences Discussions* 12, 7257-7299, doi: 10.5194/bgd-12-7257-2015, 2015.

663

664 Junet, A. de, Abril, G., Gu'erin, F., Billy, I., and Wit, R. de.: A multi-tracers analysis of
665 sources and transfers of particulate organic matter in a tropical reservoir (Petit Saut, French
666 Guiana), *River Res. Appl.*, 25, 253–271, doi:10.1002/rra.1152, 2009.

667 Kendall, C.: Tracing nitrogen sources and cycling in catchments, in: Isotope tracers in
668 catchment hydrology, edited by: Kendall, C. and McDonnell, J.J., Elsevier, Amsterdam, The
669 Netherlands, 519-576, 1998.

670

671 Kendall, C., Silva, S. R., and Kelly, V. J.: Carbon and nitrogen isotopic compositions of
672 particulate organic matter in four large river systems across the United States, *Hydrol.*
673 *Process.*, 15, 1301-1346, doi: 10.1002/hyp.216, 2001

674 Kendall, C., Elliott, E. M., and Wankel, S. D.: Tracing anthropogenic inputs of nitrogen to
675 ecosystems, Chapter 12, in: *Stable Isotopes in Ecology and Environmental Science*, edited
676 by: Michener, R. H. and Lajtha, K., 2nd Edition, Blackwell Publishing, 375-449, 2007.

677

678 Kritee, K., Sigman, D.M., Granger, J., Ward, B.B., Jayakumar, A., and Deutsch, C.: Reduced
679 isotope fractionation by denitrification under conditions relevant to the ocean, *Geochim.*
680 *Cosmochim. Acta*, 92, 243-259, doi:10.1016/j.gca.2012.05.020, 2012.

681

682 Kurian, S., Roy, R., Repeta, D.J., Gauns, M., Shenoy, D.M., Suresh, T., Sarkar, A.,
683 Narvenkar, G., Johnson, C.G., and Naqvi, S.W.A.: Seasonal occurrence of anoxygenic
684 photosynthesis in Tillari and Selaulim reservoirs, Western India, *Biogeosciences*, 9, 2485-
685 2495, doi:10.5194/bg-9-2485-2012, 2012.

686

687 Lehmann, M. F., Reichert, P., Bernasconi, S. M., Barbieri, A., and McKenzie, J.: Modelling
688 nitrogen and oxygen isotope fractionation during denitrification in a lacustrine redox-
689 transition zone, *Geochim. Cosmochim. Ac.*, 67, 2529-2542, doi: 10.1016/S0016-
690 7037(03)00085-1, 2003

691

692 Lehmann, M. F., Bernasconi, S., McKenzie, J., Barbieri, A., Simona, M., and Veronesi, M.:
693 Seasonal variation of the $\delta^{13}\text{C}$ and $\delta^{15}\text{N}$ of particulate and dissolved carbon and nitrogen in
694 Lake Lugano: Constraints on biogeochemical cycling in a eutrophic lake, *Limnol. Oceanogr.*,
695 49, 415-429, 2004.

696

697 Maya, M. V., Karapurkar, S. G., Naik, H., Roy, R., Shenoy, D. M., and Naqvi, S. W. A.: Intra-
698 annual variability of carbon and nitrogen stable isotopes in suspended organic matter in
699 waters of the western continental shelf of India, *Biogeosciences*, 8, 3441- 3456,
700 doi:10.5194/bg-8-3441-2011, 2011.

701

702 McIlvin, M. R. and Altabet, M. A.: Chemical conversion of nitrate and nitrite to nitrous oxide
703 for nitrogen and oxygen isotopic analysis in freshwater and seawater, *Anal. Chem.*, 77, 5589-
704 5595, doi: 10.1021/ac050528s, 2005.

705

706 Mengis, M., Schiff, S. L., Harris, M., English, M. C., Aravena, R., Elgood, R. J., and
707 MacLean, A.: Multiple geochemical and isotopic approaches for assessing ground water NO_3^-
708 elimination in a riparian zone, *Ground Water*, 37, 448-457, 1999.

709

710 Narvenkar, G., Naqvi, S. W. A., Kurian, S., Shenoy, D. M., Pratihary, A. K., Naik, H., Patil,
711 S., Sarkar, A., and Gauns, M.: Dissolved methane in Indian freshwater reservoirs, *Environ*
712 *Monit Assess.*, 185(8), 6989-6999, 2013.

713

714 Olleros, T.: Kinetische Isotopeneffekte der Arginase- und Nitratreduktase-Reaktion: Ein
715 Beitrag zur Aufklärung der entsprechenden Reaktionsmechanismen, Ph.D. dissertation,
716 Technische Universität München-Weihenstephan, Germany, 1983.

717
718 Pang, P. C., and Nriagu, J. O.: Isotopic variations of the nitrogen in Lake Superior, *Geochim.*
719 *Cosmochim. Acta*, 41, 811–814, doi: 10.1016/0016-7037(77)90051-5, 1977.
720
721 Prokopenko, A. A., and Williams, D.F.: Depleted methane-derived carbon in waters of Lake
722 Baikal, Siberia, *Hydrobiol.*, 544, 279-288, 2005.
723
724 Savoye, N., David, V., Morisseau, F., Etcheber, H., Abril, G., Billy, I., Charlier, K., Oggian,
725 G., Derriennic, H., and Sautour, B.: Origin and composition of particulate organic matter in a
726 macrotidal turbid estuary: the Gironde Estuary, France, *Estuar. Coast. Shelf Sci.*, 108, 16-28,
727 doi: 10.1016/j.ecss.2011.12.005, 2012.

728 Seitzinger, S. P.: Denitrification in freshwater and coastal marine ecosystems: Ecological and
729 Geochemical significance, *Limnol. Oceanogr.*, 33, 702–724, 1988.
730
731 Sigman, D. M., Robinson, R., Knapp, A. N., Van Geen, A., McCorkle, D. C., Brandes, J. A.,
732 and Thunell, R. C.: Distinguishing between water column and sedimentary denitrification in
733 the Santa Barbara Basin using the stable isotopes of nitrate. *Geochem. Geophys. Geosy.*, 4,
734 1040, doi:10.1029/2002GC000384, 2003.
735
736 Sigman, D. M., Granger, J., DiFiore, P. J., Lehmann, M. M., Ho, R., Cane, G., and van Geen,
737 A.: Coupled nitrogen and oxygen isotope measurements of nitrate along the eastern North
738 Pacific margin, *Global Biogeochem. Cy.*, 19, GB4022, doi:10.1029/2005GB002458, 2005.
739
740 Subramanya, K.: *Engineering Hydrology*, 4th edition, McGraw-Hill Publishing, New Delhi,
741 2013.
742
743 Sukumar, R., Suresh, H. S., and Ramesh, R.: Climate change and its impact on tropical
744 montane ecosystems in southern India. *J. Biogeogr.*, 22, 533-536, 1995.
745
746 Thibodeau, B., Hélie, J.-F., and Lehmann, M. F.: Variations of the nitrate isotopic
747 composition in the St. Lawrence River caused by seasonal changes in atmospheric nitrogen
748 inputs, *Biogeochemistry*, 115, 287–298, 2013.
749
750 Thunell, R. C., Sigman, D. M., Muller-Karger, F., Astor, Y., and Varela, R.: Nitrogen isotope
751 dynamics of the Cariaco Basin, Venezuela, *Global Biogeochem. Cy.*, 18, GB3001,
752 doi:10.1029/2003GB002185, 2004.
753
754 Voss, M., Dippner, J. W., and Montoya, J. P.: Nitrogen isotope patterns in the oxygen-
755 deficient waters of the Eastern Tropical North Pacific Ocean, *Deep-Sea Res. Pt. 1*, 48, 1905–
756 1921, doi:10.1016/S0967-0637(00)00110-2, 2001.
757
758 Wada, E. and Hattori, A.: Nitrogen isotope effects in the assimilation of inorganic compounds
759 by marine diatoms, *Geomicrobiol. J.*, 1, 85–101, 1978.
760
761 Wada, E.: Nitrogen isotope fractionation and its significance in biogeochemical processes
762 occurring in marine environments, in: *Isotope Marine Chemistry*, edited by: Goldberg, E. D.,
763 Horibe, Y., and Saruhashi, K., Uchida Rokakuho Pub. Co., Tokyo, 375–398, 1980.
764

765 Wankel, S. D., Kendall, C., Pennington, J. T., Chavez, F. P., and Paytan, A.: Nitrification in
766 the euphotic zone as evidenced by nitrate dual isotopic composition: Observations from
767 Monterey Bay, California, *Global Biogeochem. Cy.*, 21, GB2009,
768 doi:10.1029/2006gb002723, 2007.

769

770 Wenk, C. B., Zopfi, J., Bles, J., Veronesi, M., Niemann, H., and Lehmann, M. F.:
771 Community N and O isotope fractionation by sulfide-dependent denitrification and anammox
772 in a stratified lacustrine water column, *Geochim. Cosmochim. Acta*, 125, 551-563, 2014.

773 Whiticar, M. J., Faber, E., and Schoell, M.: Biogenic methane formation in marine and
774 freshwater environments:CO₂ reduction vs. acetate fermentation-isotope evidence, *Geochim*
775 *Cosmochim Acta*, 50, 693-709, 1986.

776

777

778

779

780

781

782

783

784

785

786

787

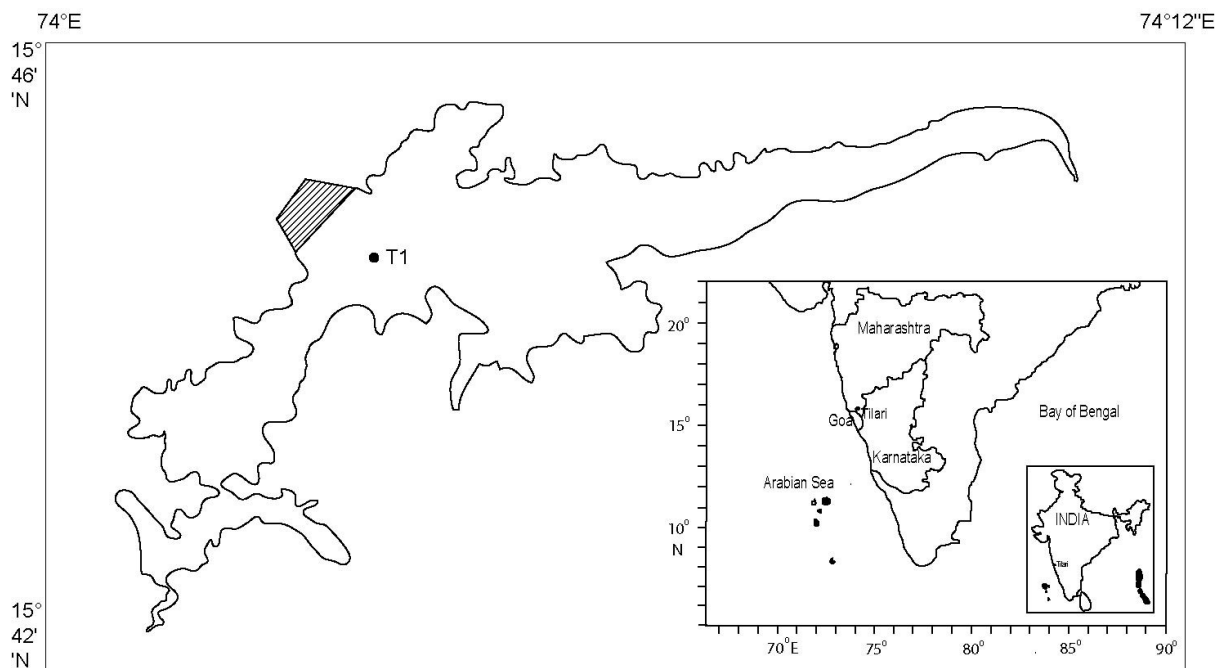
788 Table 1: The values of nitrogen (ϵ^{15}) and oxygen (ϵ^{18}) isotope effects for denitrification as
 789 reported from some natural systems as well as laboratory cultures.

790
 791

| Study Area | ϵ^{15} (‰) | ϵ^{18} (‰) | Reference |
|--------------------------------|---------------------|---------------------|-------------------|
| Cariaco Basin, Venezuela | | | |
| Beijiang River, China | | 8.5 | |
| Boknis Eck, Baltic Sea | | 15.8 | |
| Lake Lugano, Switzerland | | 6.6 | |
| Groundwater | | 18.3 | |
| Denitrifier culture | | 15 | |
| Denitrifier culture | | | |
| Open-ocean OMZs | | | |
| Shallow groundwater aquifer | | 8 | |
| Tillari reservoir, India | 8.73 | 10.74 | This study |

792
 793
 794
 795
 796
 797
 798
 799
 800
 801
 802
 803
 804
 805
 806
 807
 808
 809
 810
 811

812 **Figure 1: Map of the sampling location (Tillari Reservoir). T1 shows the main sampling**
813 **location at the deepest point of the reservoir.**



814

815

816

817

818

819

820

821

822

823

824

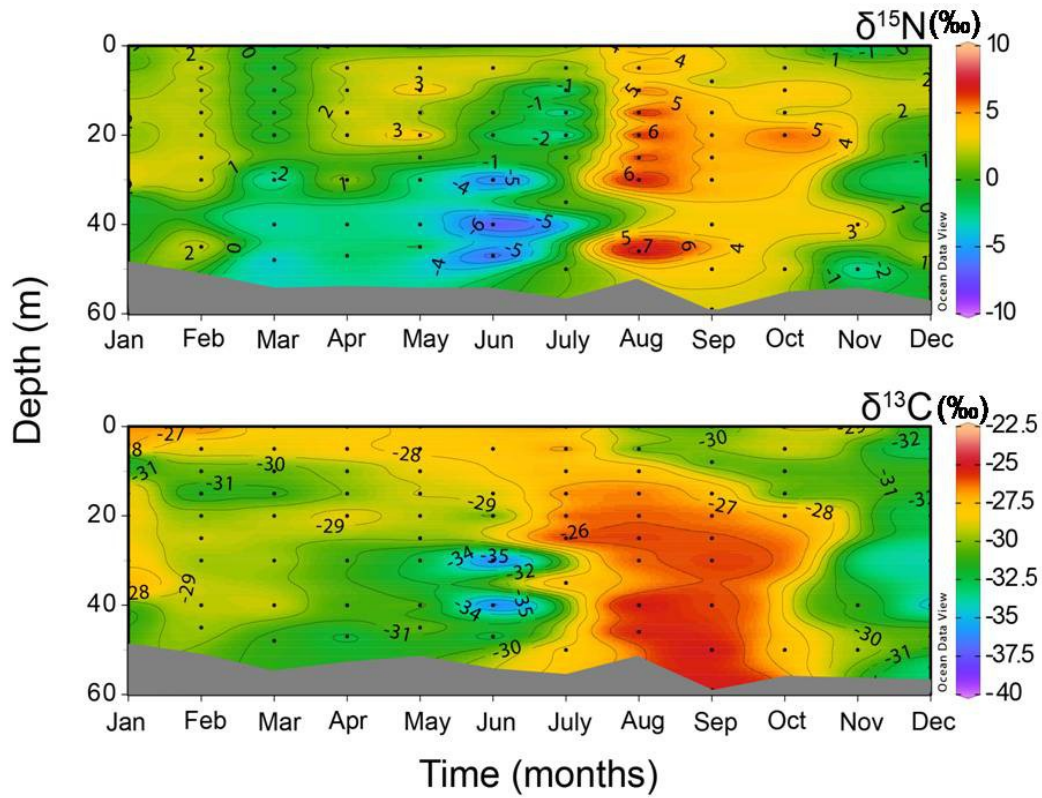
825

826

827

828

829 **Figure 2: Mean annual variations of $\delta^{15}\text{N-POM}$ and $\delta^{13}\text{C-POM}$ at the main sampling**
830 **location.**



831

832

833

834

835

836

837

838

839

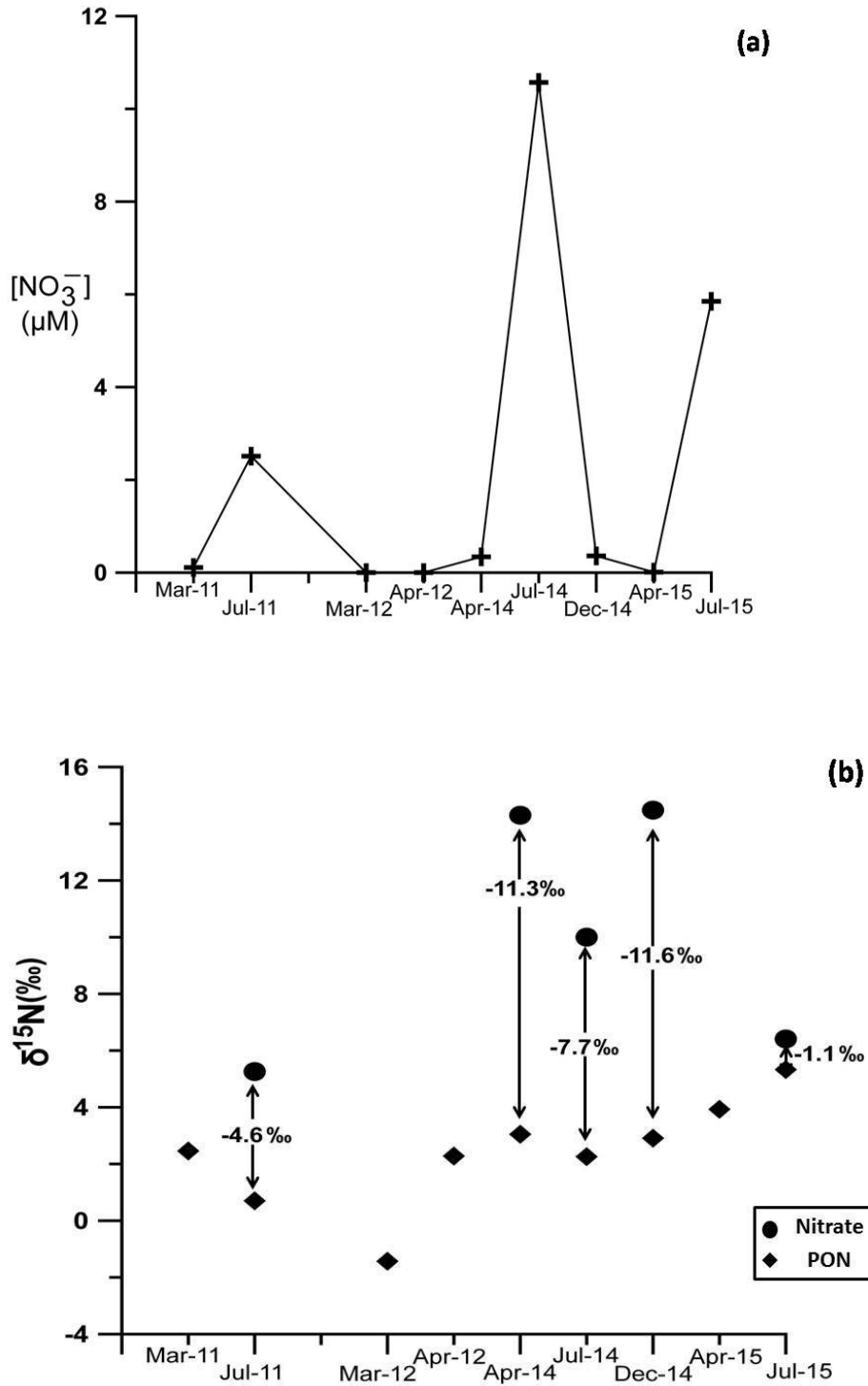
840

841

842

843

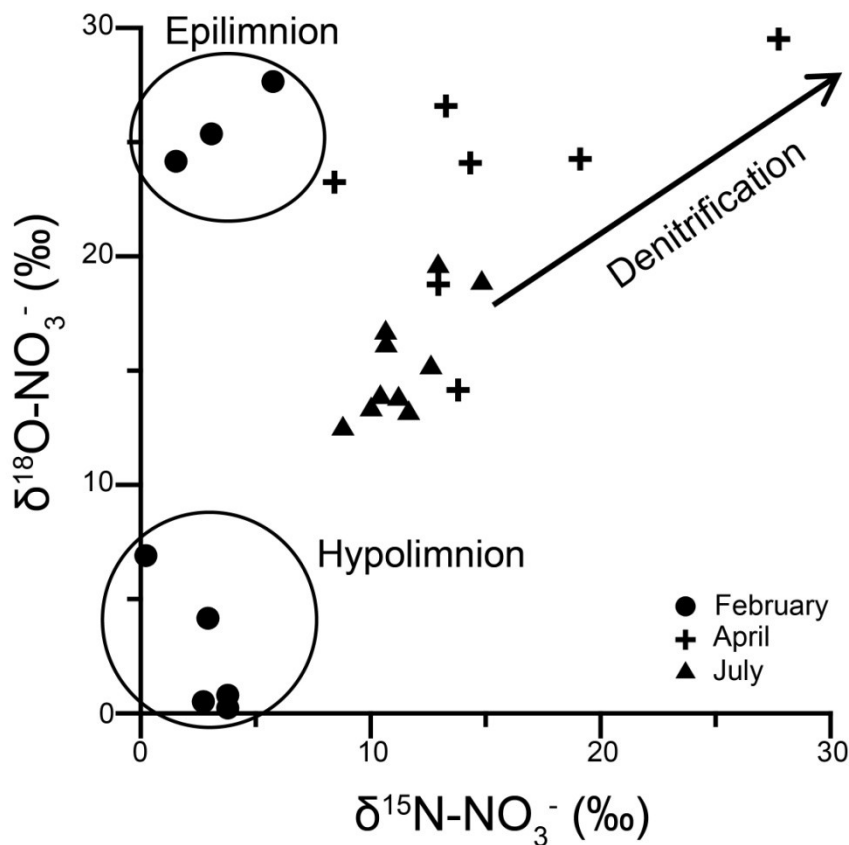
844 **Figure 3: Time-series of nitrate concentrations (a) and $\delta^{15}\text{N}$ of dissolved nitrate and**
 845 **POM in the epilimnion (0-5 m) (b). The isotopic differences between the dissolved and**
 846 **particulate species have been denoted by arrows. Each data point represents one**
 847 **sample. Each data point represents a single sample.**



848

849

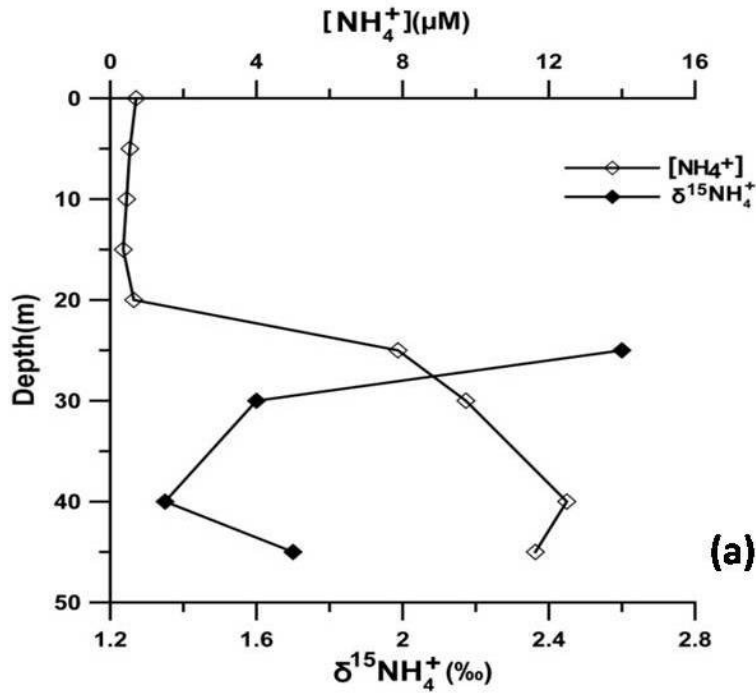
850 **Figure 4: Nitrogen and oxygen isotopic composition of dissolved nitrate during three**
851 **different periods in 2014. February represents the early or weak stratification period**
852 **with two distinct clusters of epilimnetic (0-10 m) and hypolimnetic (15-48 m) samples.**
853 **April is a period of intense water-column stratification and denitrification signal is**
854 **observed in the bottom waters. July is a period of monsoon holomixis when the water**
855 **column has uniformly high nitrate values.**



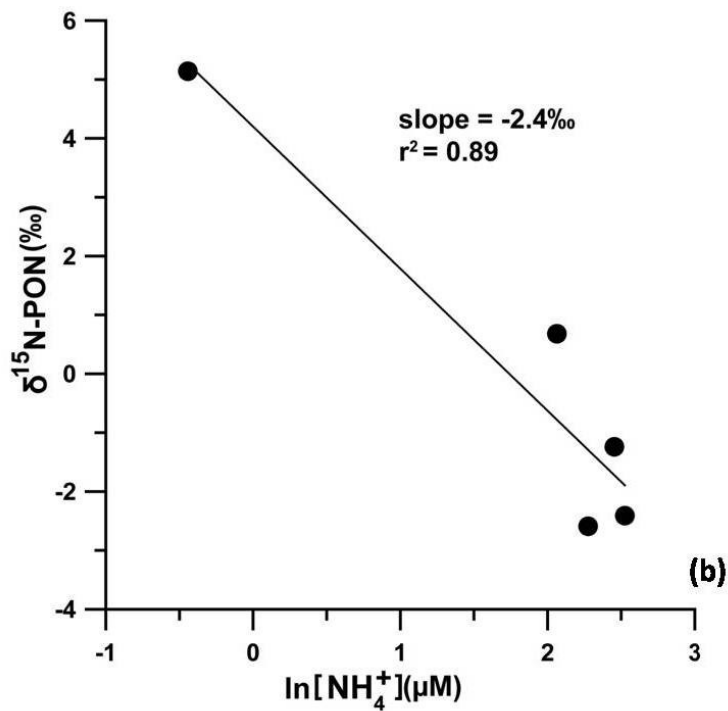
856
857
858
859
860
861
862

863 Figure 5: (a) Depth-wise variations of ammonium concentration and $\delta^{15}\text{N-NH}_4^+$ in May
 864 2012. (b) Plot of $\delta^{15}\text{N-PON}$ versus $\ln(\text{NH}_4^+)$. The negative linear correlation yields a
 865 fractionation factor (ϵ) of -2.4‰. Each data point represents a single sample.

866

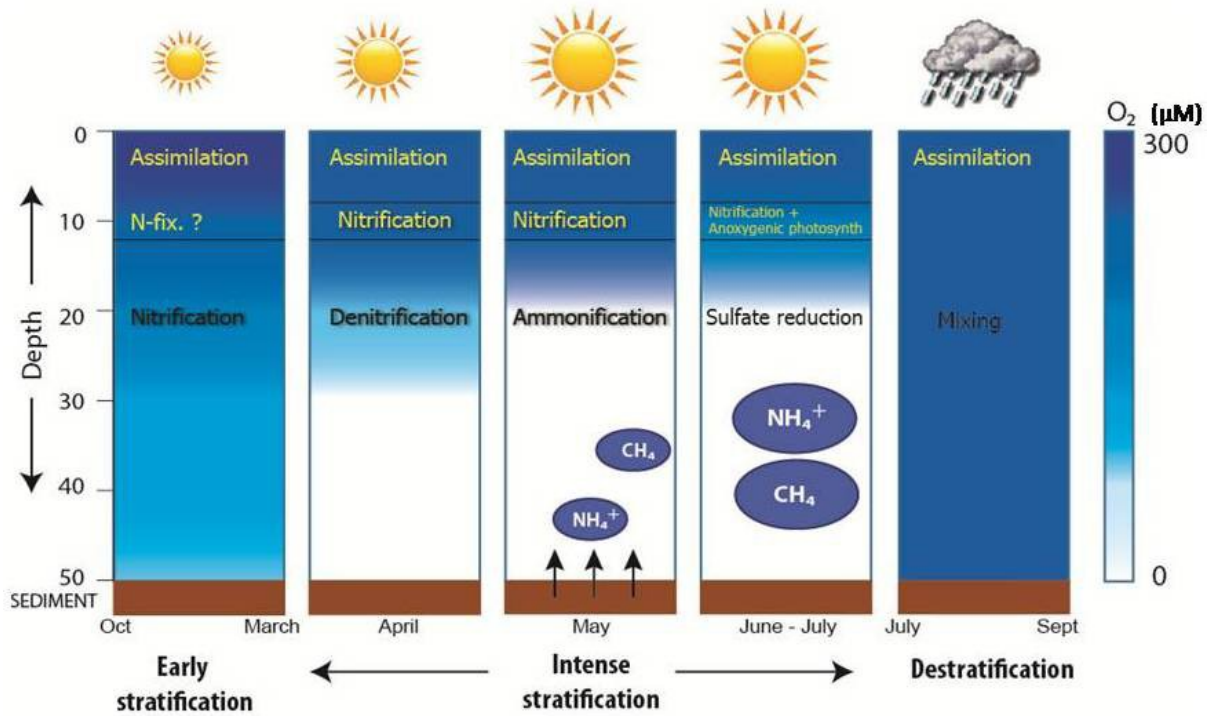


867



868

869 **Figure 6: Schematic diagram depicting major biogeochemical processes taking place in**
 870 **the Tillari Reservoir over an annual cycle. This information is based on monthly**
 871 **sampling in the reservoir for several years (Shenoy et al., manuscript in preparation)**



872

873

874

875

876

877

878

879

880

881

882

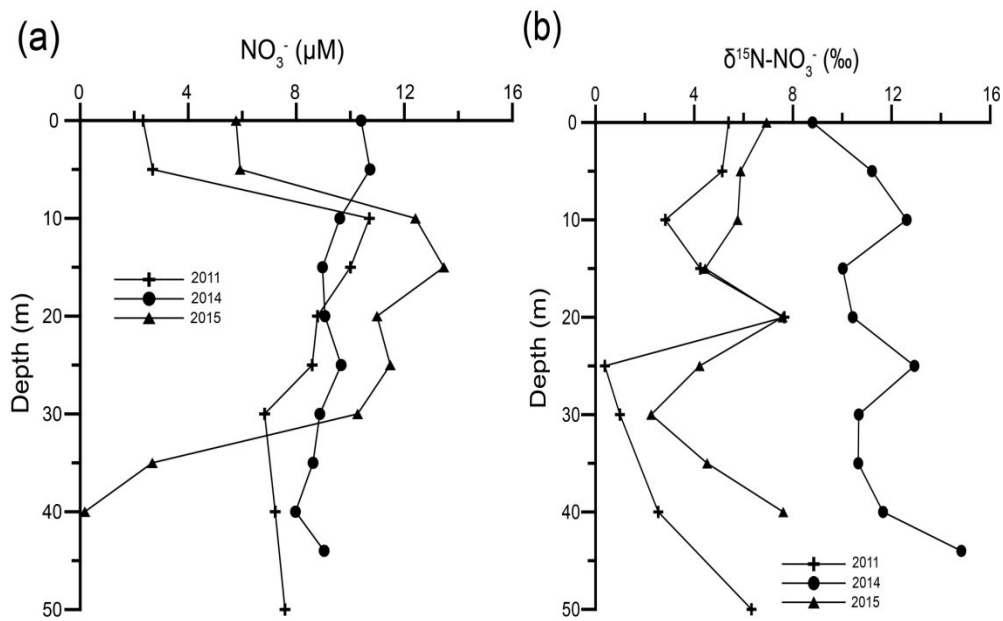
883

884 **Figure 7: Vertical profiles of NO_3^- (a) and $\delta^{15}\text{N}\text{-NO}_3^-$ (b) during monsoon mixing in 2011,**
885 **2014 and 2015. Each profile is from one field trip during the peak SWM in a given year**
886 **with each data point representing one sample.**

887

888

889



890